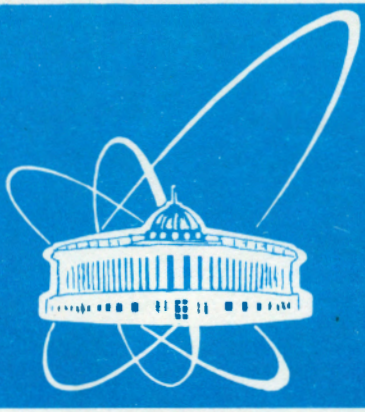

ОБЪЕДИНЕННЫЙ
ИНСТИТУТ
ЯДЕРНЫХ
ИССЛЕДОВАНИЙ

Дубна

E17-98-244

N.M.Plakida, V.S.Oudovenko

ELECTRON SPECTRUM AND SUPERCONDUCTIVITY IN THE $t-J$ MODEL AT MODERATE DOPING

Submitted to «Physical Review B»

1998

1 INTRODUCTION

Experimental studies of high-temperature superconductors have provided strong support for a major role of strong electron correlations in copper-oxide materials (see, e.g., [1]). Many anomalous normal state properties have been explained within the models with strong electron correlations as it first has been proposed by Anderson [2, 3]. However, the origin of the d-wave superconducting pairing is still under discussion [4]. Presently we have no rigorous methods to study these models for dimensions $d \geq 2$ to find an unambiguous solution of the problem. The recently developed dynamical mean field theory (for reviews see [5, 6]) being exact in the infinite dimensions has been successfully applied to study the Mott-Hubbard transition and normal state properties within the Hubbard model where local correlations are the most important. However, the theory is unable to treat properly nonlocal correlations as e.g., exchange interaction in the $t-J$ model and the nonlocal d-wave type superconducting pairing.

To deal with the strong coupling limit for the Hubbard model and the $t-J$ model a number of numerical methods for finite clusters has been developed (for reviews see [7], [4]). These studies show strong antiferromagnetic correlations which lead to the formation of the $d_{x^2-y^2}$ pairing correlations. However, the finite cluster calculations due to known limitations (finite size effects, few filling fractions, etc.) can give only restricted information. For instance, as it was shown recently by applying the constrained-path Monte Carlo method [8] to the two-dimensional Hubbard model, small lattice sizes and weak interactions show $d_{x^2-y^2}$ pairing correlations while with increasing lattice size or interaction they vanish. So to prove superconducting pairing in the strong coupling limit an analytical treatment is highly demanded.

In the limit of a low electron density a t-matrix approach can be used to study the $t-J$ model. In [9] the authors observed various forms of electron pairing at low temperatures including the d-wave instability at large values of $J/t > 1$. By combining a generalized Lanczos scheme with the variational Monte Carlo method in the $t-J$ model, a finite d-wave long-range superconducting order was observed below the phase-separation region [10].

The main problem in studies of the $t-J$ model is the so-called kinematical interaction imposed by the projected character of electron operators acting in the subspace of singly occupied lattice sites. To take into account the constraints of no double occupancy different types of slave-boson (-fermion) technique were proposed (see [11]-[14] and references therein). In the mean field approximation (MFA) the local constraints are approximated by a global one, that reduces the problem to free fermions and bosons in the mean field [11]. To treat the constraints in a systematic way, in [12], [13] a large-N expansion, with N being a number of states (orbitals) at a lattice site, was used. In that approach the local constraints are relaxed and a weak coupling approximation is possible. By using the $1/N$ expansion, the d-wave superconducting instability induced by the exchange interaction was obtained in the $t-J$ model close to half filling [13].

Another method is based on the Baym-Kadanoff variational technique for the Green functions in terms of the Hubbard operators [15]. The method was used in [16, 17], also in the limit of large N, to consider superconducting pairing in the $t-J$ model. It was shown that in the lowest order of $1/N$ there is a strong compensation of different contributions to the pairing interaction and for $J = 0$ the superconducting T_c is extremely small. For a finite J the d-wave superconducting instability mediated by exchange and charge fluctuations was obtained below $T_c \simeq 0.01t$. However, in the large-N expansion the kinematical interaction is suppressed and this approach, being rigorous in the limit $N \to \infty$, is difficult to extrapolate to real spin systems with $N = 2$.

A formally rigorous method to treat the unconventional commutation relations for the projected electron operators is based on the diagram technique for the Hubbard operators [18], [19] since in this method the local constraints are rigorously implemented by the Hubbard operator algebra. A superconducting pairing due to the kinematical interaction in the Hubbard model in the limit of strong electron correlations ($U \to \infty$) was first obtained by Zaitsev and Ivanov [20] who studied the lowest order diagrams for a two-particle vertex equation. Their approximation, being equivalent to the MFA for a superconducting order parameter, gives only the s-wave pairing. Close results were obtained for the Hubbard model in [21, 22] by applying the equation of motion method for the Green functions. However, as was shown later [23, 24], the s-wave pairing in the limit of strong correlations violates an exact requirement of no single-site pairs and should be rejected. In [23, 24] the BCS mean field theory for the $t-J$ model was developed within the formally exact projection technique [25] for the Green functions in terms of the Hubbard operators. It was proved that the d-wave superconducting pairing mediated by the exchange interaction is thermodynamically stable and has high $T_c \simeq 0.1t$ for $J \simeq 0.4t$.

On the basis of the diagram technique, detailed studies of spin fluctuations and superconducting pairing in the $t-J$ model were performed by Izyumov et al. [26]. Summation of the first order diagrams for the self-energy reproduced the results of the MFA in [23, 24]. In the second order diagrams only the exchange interaction J was taken into account while the corresponding contributions due to the kinematical interaction t were disregarded. Estimations done in the weak coupling limit for the Eliashberg equation revealed quite a low superconducting T_c. The diagram technique for the Hubbard operators was also used in [27, 28] where the BCS equation in the MFA was obtained. In [28] the s-wave and d-wave solutions were studied for a model with large FS.

In the limit of small hole concentrations one can consider a one-hole motion on the antiferromagnetic background within the spin-polaron representation for the $t-J$ model [29, 30]. A number of studies of this model (see, e.g., [31] - [37] and references therein) predicts that a doped hole dressed by antiferromagnetic spin fluctuations can propagate coherently as a spin-polaron quasi-particle (QP) even for a finite hole doping [33, 34]. It was suggested that the same spin fluctuations could mediate a superconducting pairing of the spin-polaron QP. This problem was treated in the

framework of the weak coupling BCS formalism for a phenomenological model of QP with numerically evaluated spectrum [38], [39]. A self-consistent numerical solution of the strong coupling Eliashberg equations for spin-polarons and magnons in the $t-J$ model has been given in [40]. A strong renormalization of the hole spectrum due to spin-fluctuations and the d- wave pairing of spin-polaron QP with maximum $T_c \simeq 0.01t$ were obtained. In Ref. [41] the superconducting instability within the spin-polaron model was obtained only with additional electron-phonon coupling.

However, numerical studies [42] of the 2D $t-J$ model at moderate doping have questioned the single-hole QP picture developed within the spin-polaron model for the superconducting paramagnetic regime. To elucidate the problem, in the present paper we propose a theory of electron spectrum and superconducting pairing for the $t-J$ model in paramagnetic state by applying the projection technique [25] for the Green functions [43] in terms of the Hubbard operators. A formally exact representation for the Dyson equation with the self-energy as the many-particle Green function is derived. By using the noncrossing approximation, numerical solution of the self-consistent system of the Eliashberg equations is performed. We observe narrow QP peaks for the single-electron spectral density near the Fermi surface (FS) and a broad incoherent band below the Fermi level. The incoherent part of the spectrum results in nonzero occupation numbers $N(\mathbf{k})$ throughout the Brillouin zone. In that respect our results are in a reasonable agreement with numerical studies [42]. A direct numerical solution of the linearized gap equation reveals the d-wave superconducting instability and high T_c at optimal doping. These results are in accord with the previous calculations for the spin-polaron $t-J$ model [40].

The paper is organized as follow. In the next, Sec. II, we present the Dyson equation for the matrix Green function in terms of the Hubbard operators. In Sec. III a self-consistent system of the Eliashberg equations in the noncrossing (self-consistent) approximation is formulated. In Sec. IV numerical results for the single-electron spectral density, occupation numbers $N(\mathbf{k})$, a superconducting gap function, and T_c are analyzed. Conclusions are given in Sec. V.

2 DYSON EQUATION FOR THE t-J MODEL

We consider the $t-J$ model in the standard notation [2, 44]:

$$H_{t-J} = -t\sum_{i\neq j,\sigma}\tilde{a}^{+}_{i\sigma}\tilde{a}_{j\sigma} + J\sum_{\langle ij\rangle}(\mathbf{S}_i\mathbf{S}_j - \frac{1}{4}n_in_j), \tag{1}$$

where $\tilde{a}^{+}_{i\sigma} = a^{+}_{i\sigma}(1-n_{i-\sigma})$ are projected electron operators and $S^{\alpha}_i = (1/2)\sum_{s,s'}\tilde{a}^{+}_{is}\sigma^{\alpha}_{s,s'}\tilde{a}_{is'}$ are spin-1/2 operators. Here t is an effective transfer integral and J is the antiferromagnetic exchange energy for a pair of nearest neighbor sites, $\langle ij\rangle$, $i>j$.

To take into account on a rigorous basis the projected character of electron operators we employ the Hubbard operator (HO) technique [45]. The HO are defined

as

$$X^{\alpha\beta}_i = |i,\alpha\rangle\langle i,\beta| \tag{2}$$

for three possible states at a lattice site i: $|i,\alpha\rangle = |i,0\rangle$, $|i,\sigma\rangle$ for an empty site and for a singly occupied site by an electron with spin $\sigma/2$ ($\sigma = \pm 1$, $\bar{\sigma} = -\sigma$). They obey the completeness relation

$$X^{00}_i + \sum_{\sigma} X^{\sigma\sigma}_i = 1, \tag{3}$$

which rigorously preserves the constraint of no double occupancy.

The spin and density operators in Eq.(1) are expressed by HO as

$$S^{\sigma}_i = X^{\sigma\bar{\sigma}}_i, \quad S^{z}_i = \frac{1}{2}\sum_{\sigma}\sigma X^{\sigma\sigma}_i, \quad n_i = \sum_{\sigma} X^{\sigma\sigma}_i. \tag{4}$$

The HO obey the following multiplication rules

$$X^{\alpha\beta}_i X^{\gamma\delta}_i = \delta_{\beta\gamma}X^{\alpha\delta}_i, \tag{5}$$

and commutation relations

$$\left[X^{\alpha\beta}_i, X^{\gamma\delta}_j\right]_{\pm} = \delta_{ij}\left(\delta_{\beta\gamma}X^{\alpha\delta}_i \pm \delta_{\delta\alpha}X^{\gamma\beta}_i\right). \tag{6}$$

In Eq.(6) the upper sign stands for the case when both HO are the Fermi-like ones (as, e. g., $X^{0\sigma}_i$). The spin and density operators (4) are the Bose-like and for them the lower sign in Eq.(6) should be taken.

By using the Hubbard operator representation (2) for $\tilde{a}^{+}_{i\sigma} = X^{\sigma 0}_i$ and $\tilde{a}_{j\sigma} = X^{0\sigma}_j$ and (4) for spin and number operators we write the Hamiltonian of the $t-J$ model (1) in a more general form:

$$H_{t-J} = -\sum_{i\neq j,\sigma} t_{ij}X^{\sigma 0}_i X^{0\sigma}_j - \mu\sum_{i\sigma} X^{\sigma\sigma}_i$$

$$+\frac{1}{4}\sum_{i\neq j,\sigma} J_{ij}\left(X^{\sigma\bar{\sigma}}_i X^{\bar{\sigma}\sigma}_j - X^{\sigma\sigma}_i X^{\bar{\sigma}\bar{\sigma}}_j\right). \tag{7}$$

The electron hopping energy for the nearest neighbors, $t_{ij} = t$, and the second neighbors, $t_{ij} = t'$, on a 2D square lattice, and the exchange interaction $J_{ij} = J$ for the nearest neighbors can be considered as independent parameters if, starting from a more realistic for copper oxides three-band $p-d$ model, we reduce it to the $t-J$ model [44]. In that case the parameters t, t' and J can be evaluated in terms of the original parameters of the $p-d$ model (see, e.g., [46], [36], [37]). We introduced also the chemical potential μ which can be calculated from the equation for the average number of electrons

$$n = \sum_{i,\sigma}\langle X^{\sigma\sigma}_i\rangle. \tag{8}$$

To discuss the superconducting pairing within the model (7) we consider the matrix Green function (GF)

$$\hat{G}_{ij,\sigma}(t-t') = \langle\langle \Psi_{i\sigma}(t) | \Psi^{+}_{j\sigma}(t') \rangle\rangle \tag{9}$$

in terms of the Nambu operators:

$$\Psi_{i\sigma} = \begin{pmatrix} X_i^{0\sigma} \\ X_i^{\bar{\sigma}0} \end{pmatrix}, \qquad \Psi^{+}_{i\sigma} = \left(X_i^{\sigma 0} \; X_i^{0\bar{\sigma}} \right) , \tag{10}$$

where Zubarev's notation for the anticommutator Green function (9) is used [43].

By differentiating the GF (9) over the time t we get for the Fourier component the following equation

$$\omega \hat{G}_{ij\sigma}(\omega) = \delta_{ij} \hat{Q}_{\sigma} + \langle\langle \hat{Z}_{i\sigma} \mid \Psi_{j\sigma} \rangle\rangle_{\omega}, \tag{11}$$

where $\hat{Z}_{i\sigma} = [\Psi_{i\sigma}, H]$, $\hat{Q}_{\sigma} = \begin{pmatrix} Q_{\sigma} & 0 \\ 0 & Q_{\bar{\sigma}} \end{pmatrix}$ with $Q_{\sigma} = \langle X_i^{00} + X_i^{\sigma\sigma} \rangle$. Since we consider a spin-singlet state the correlation function $Q_{\sigma} = Q = 1 - n/2$ depends only on the average number of electrons (8).

Now, we project the many–particle GF in (11) on the single–electron GF by introducing the irreducible (irr) part of $\hat{Z}_{i\sigma}$ operator

$$\langle\langle \hat{Z}_{i\sigma} \mid \Psi^{+}_{j\sigma} \rangle\rangle = \sum_{l} \hat{E}_{il\sigma} \langle\langle \Psi_{l\sigma} \mid \Psi^{+}_{j\sigma} \rangle\rangle + \langle\langle \hat{Z}^{(irr)}_{i\sigma} \mid \Psi^{+}_{j\sigma} \rangle\rangle,$$

$$\langle \{ \hat{Z}^{(irr)}_{i\sigma}, \Psi^{+}_{j\sigma} \} \rangle = \langle \hat{Z}^{(irr)}_{i\sigma} \Psi^{+}_{j\sigma} + \Psi^{+}_{j\sigma} \hat{Z}^{(irr)}_{i\sigma} \rangle = 0, \tag{12}$$

that results in the equation for the frequency matrix

$$\hat{E}_{ij\sigma} = \langle \{ [\Psi_{i\sigma}, H], \Psi^{+}_{j\sigma} \} \rangle \, Q^{-1} : \tag{13}$$

To calculate the matrix (13) we use the equation of motion for the HO:

$$\left(i\frac{d}{dt} + \mu \right) X_i^{0\sigma} = -\sum_{l} t_{il} B_{i\sigma\sigma'} X_l^{0\sigma'}$$

$$+ \frac{1}{2} \sum_{l} J_{il} (B_{l\sigma\sigma'} - \delta_{\sigma\sigma'}) X_i^{0\sigma'}, \tag{14}$$

where we introduced the operator

$$B_{i\sigma\sigma'} = (X_i^{00} + X_i^{\sigma\sigma}) \delta_{\sigma'\sigma} + X_i^{\bar{\sigma}\sigma} \delta_{\sigma'\bar{\sigma}}$$

$$= (1 - \frac{1}{2} N_i + \sigma S_i^z) \delta_{\sigma'\sigma} + S_i^{\bar{\sigma}} \delta_{\sigma'\bar{\sigma}}. \tag{15}$$

The Bose-like operator (15) describes electron scattering on spin and charge fluctuations caused by the nonfermionic commutation relations for the HO (the first term

in (14) – the kinematical interaction) and by the exchange spin-spin interaction (the second term in (14)).

Now we introduce the zero–order GF in the generalized MFA which is given by the frequency matrix (13)

$$\hat{G}^{0}_{ij\sigma}(\omega) = Q \{ \omega \hat{\tau}_0 \delta_{ij} - \hat{E}_{ij\sigma} \}^{-1}. \tag{16}$$

By writing the equation of motion for the irreducible part of the GF in (12) with respect to the second time t' for the right–hand side operator $\Psi^{+}_{j\sigma}(t')$ and performing the same projection procedure as in (12) we can obtain the Dyson equation for the GF (9) in the form

$$\hat{G}_{ij\sigma}(\omega) = \hat{G}^{0}_{ij\sigma}(\omega) + \sum_{kl} \hat{G}^{0}_{ik\sigma}(\omega) \; \hat{\Sigma}_{kl\sigma}(\omega) \; \hat{G}_{lj\sigma}(\omega), \tag{17}$$

where the self–energy operator $\hat{\Sigma}_{kl\sigma}(\omega)$ is defined by the equation

$$\hat{T}_{ij\sigma}(\omega) = \hat{\Sigma}_{ij\sigma}(\omega) + \sum_{kl} \hat{\Sigma}_{ik\sigma}(\omega) \; \hat{G}^{0}_{kl\sigma}(\omega) \; \hat{T}_{lj\sigma}(\omega) \, . \tag{18}$$

Here the scattering matrix is given by

$$\hat{T}_{ij\sigma}(\omega) = Q^{-1} \langle\langle \hat{Z}^{(irr)}_{i\sigma} \mid \hat{Z}^{(irr)^{+}}_{j\sigma} \rangle\rangle_{\omega} \, Q^{-1} \, . \tag{19}$$

From Eq. (18) it follows that the self-energy operator is given by the irreducible part of the scattering matrix (19) that has no parts connected by the single zero-order GF (16):

$$\hat{\Sigma}_{ij\sigma}(\omega) = Q^{-1} \langle\langle \hat{Z}^{(irr)}_{i\sigma} \mid \hat{Z}^{(irr)^{+}}_{j\sigma} \rangle\rangle^{(irr)}_{\omega} \, Q^{-1} \, . \tag{20}$$

Eqs. (16), (17) and (20) give an exact representation for the single–electron GF (9). To calculate it, however, one has to introduce an approximation for the many–particle GF in the self-energy matrix (20) which describes inelastic scattering of electrons on spin and charge fluctuations.

3 SELF-CONSISTENT ELIASHBERG EQUATIONS

In the k-representation for the GF

$$G^{\alpha\beta}_{\sigma}(k,\omega) = \sum_{j} G^{\alpha\beta}_{oj\sigma}(\omega) \; \mathrm{e}^{-\mathbf{ikj}} \, , \tag{21}$$

we get for the zero-order GF (16):

$$\hat{G}^{(0)}_{\sigma}(k,\omega)^{-1} = \{ \omega \hat{\tau}_0 - (E^{\sigma}_{k} - \tilde{\mu}) \hat{\tau}_3 - \Delta^{\sigma}_{k} \hat{\tau}_1 \} Q^{-1}, \tag{22}$$

where $\hat{\tau}_0$, $\hat{\tau}_1$, $\hat{\tau}_3$ are the Pauli matrices. The energy of the quasiparticles E_k^σ, the renormalized chemical potential $\tilde{\mu} = \mu - \delta\mu$ and the gap function Δ_k^σ in the MFA (13) are given by

$$E_k^\sigma = -\epsilon(k)Q - \epsilon_s(k)/Q - \frac{2J}{N}\sum_q \gamma(k-q)N_{q\sigma}, \tag{23}$$

where we have introduced $J(q) = 4J\gamma(q)$ and

$$\epsilon(k) = t(k) = 4t\gamma(k) + 4t'\gamma'(k)\,,$$

$$\epsilon_s(k) = 4t\gamma(k)\chi_{1s} + 4t'\gamma'(k)\chi_{2s},$$

with $\gamma(k) = (1/2)(\cos a_x q_x + \cos a_y q_y)$ and
$\gamma'(k) = \cos a_x q_x \cos a_y q_y$,

$$\delta\mu = \frac{1}{N}\sum_q \epsilon(q)N_{q\sigma} - 2J(\frac{n}{2} - \frac{\chi_{1s}}{Q})\,, \tag{24}$$

$$\Delta_k^\sigma = -\frac{2}{NQ}\sum_q g(q, k-q)\,\langle X_{-q}^{0\bar{\sigma}} X_q^{0\sigma}\rangle, \tag{25}$$

where the interaction is given by the function:

$$g(q, k-q) = t(q) - \frac{1}{2}J(k-q). \tag{26}$$

There are two contributions in the gap equation (25): the k-independent kinematical interaction $t(q)$ and the exchange interaction $J(k-q)$. The kinematical interaction gives no contribution to the d-wave pairing in MFA, Eq. (25)(see [23]), and we disregard it in the following equations. The average number of electrons in Eqs. (23), (24) in the k-representation is written in the form:

$$n_{k,\sigma} = \langle X_k^{\sigma 0} X_k^{0\sigma}\rangle = QN_{k\sigma}\,. \tag{27}$$

In calculation of the normal part of the frequency matrix (23) we have neglected the charge fluctuation and introduced the spin correlation functions for the nearest (χ_{1s}) and the next-nearest (χ_{2s}) neighbor lattice sites

$$\chi_{1s} = \langle \mathrm{S}_i \mathrm{S}_{i+a_1}\rangle\,, \quad \chi_{2s} = \langle \mathrm{S}_i \mathrm{S}_{i+a_2}\rangle, \tag{28}$$

where $a_1 = (\pm a_x, \pm a_y)$ and $a_2 = \pm(a_x \pm a_y)$ are the nearest and the next-nearest neighbor lattice sites.

To calculate the self-energy operator we employ the noncrossing approximation (or the self-consistent Born approximation) for the irreducible part of the many particle Green function in (20). For the two-time GF the noncrossing approximation is given by the two-time decoupling for the corresponding correlation functions in (20):

$$\langle X_{j'}^{\sigma' 0} B_{j\sigma\sigma'}^+ X_{i'}^{0\sigma'}(t) B_{i\sigma\sigma'}(t)\rangle$$

$$\simeq \langle X_{j'}^{\sigma' 0} X_{i'}^{0\sigma'}(t)\rangle\langle B_{j\sigma\sigma'}^+ B_{i\sigma\sigma'}(t)\rangle\,. \tag{29}$$

The proposed decoupling does not violate equal time correlations since in Eq. (29) $j \neq j'$ and $i \neq i'$. Using the spectral representation for the GF, we obtain in the noncrossing approximation the following expression for the normal and anomalous components of the self-energy, $\tilde{\Sigma}_{\alpha\beta}(k,\omega) = Q\hat{\Sigma}_{\alpha\beta}(k,\omega)$:

$$\tilde{\Sigma}_{11}^\sigma(k,\omega) = -\tilde{\Sigma}_{22}^{\bar{\sigma}}(-k,-\omega) =$$

$$= \frac{1}{N}\sum_q \int\int_{-\infty}^{+\infty} dz d\Omega N(\omega, z, \Omega)\lambda_{11}(q, k-q \mid \Omega)A_{11}^\sigma(q,z), \tag{30}$$

$$\tilde{\Sigma}_{12}^\sigma(k,\omega) = (\tilde{\Sigma}_{21}^\sigma(k,\omega))^* =$$

$$= \frac{1}{N}\sum_q \int\int_{-\infty}^{+\infty} dz d\Omega N(\omega, z, \Omega)\lambda_{12}(q, k-q \mid \Omega)A_{12}^\sigma(q,z), \tag{31}$$

where

$$N(\omega, z, \Omega) = \frac{1}{2}\frac{\tanh(z/2T) + \coth(\Omega/2T)}{\omega - z - \Omega}. \tag{32}$$

Here we introduce the spectral density:

$$A_{11}^\sigma(q,z) = -\frac{1}{Q\pi}\mathrm{Im}\,\langle\langle X_q^{0\sigma} \mid X_q^{\sigma 0}\rangle\rangle_{z+i\delta}, \tag{33}$$

$$A_{12}^\sigma(q,z) = -\frac{1}{Q\pi}\mathrm{Im}\,\langle\langle X_q^{0\sigma} \mid X_{-q}^{0\bar{\sigma}}\rangle\rangle_{z+i\delta}, \tag{34}$$

and the electron – electron interaction functions caused by spin-charge fluctuations

$$\lambda_{11}(q, k-q \mid \Omega) =$$

$$= g^2(q, k-q)[-\frac{1}{\pi}\mathrm{Im}\,D^+(k-q, \Omega + i\delta)], \tag{35}$$

$$\lambda_{12}(q, k-q \mid \Omega) =$$

$$= g^2(q, k-q)[-\frac{1}{\pi}\mathrm{Im}\,D^-(k-q, \Omega + i\delta)], \tag{36}$$

where the spectral density for the spin-charge fluctuations is defined by the boson-like commutator GF

$$D^\pm(q,\Omega) = \langle\langle \mathrm{S}_q \mid \mathrm{S}_{-q}\rangle\rangle_\Omega \pm \frac{1}{4}\langle\langle n_q \mid n_q^+\rangle\rangle_\Omega. \tag{37}$$

The solution of the Dyson equation (17) can be written in the Eliashberg notation as

$$\hat{G}^\sigma(k,\omega) = Q\tilde{G}^\sigma(k,\omega)$$

$$= Q\frac{\omega Z_k^\sigma(\omega)\hat{\tau}_0 + (E_k^\sigma + \xi_k^\sigma(\omega) - \tilde{\mu})\hat{\tau}_3 + \Phi_k^\sigma(\omega)\hat{\tau}_1}{(\omega Z_k^\sigma(\omega))^2 - (E_k^\sigma + \xi_k^\sigma(\omega) - \tilde{\mu})^2 - \mid \Phi_k^\sigma(\omega) \mid^2}, \tag{38}$$

where

$$\omega(1 - Z_k^\sigma(\omega)) = \frac{1}{2}[\tilde{\Sigma}_{11}^\sigma(k,\omega) + \tilde{\Sigma}_{22}^\sigma(k,\omega)] \,,$$

$$\xi_k^\sigma(\omega) = \frac{1}{2}[\tilde{\Sigma}_{11}^\sigma(k,\omega) - \tilde{\Sigma}_{22}^\sigma(k,\omega)] \,, \tag{39}$$

$$\Phi_k^\sigma(\omega) = \Delta_k^\sigma + \tilde{\Sigma}_{12}^\sigma(k,\omega) \,,$$

and, by fixing the phase of the gap function, we take it to be real.

4 NUMERICAL RESULTS AND DISCUSSION

For numerical solution of the system of equations (30) - (39) we have used the imaginary frequency representation for the Green function (38) with $\omega = i\omega_n = i\pi T(2n+1)$ and the spin-charge Green function (37) with $\Omega = i\omega_n = i\pi T 2n$ where $n = 0, \pm 1, \pm 2, \ldots$. By using the representation for the function (32)

$$N(i\omega_n, z, \Omega) = -T\sum_m \frac{1}{i\omega_m - z} \quad \frac{1}{i(\omega_n - \omega_m) - \Omega} \tag{40}$$

after integration in Eqs. (30), (31) we get

$$\tilde{\Sigma}_{11}^\sigma(k, i\omega_n) =$$

$$= -\frac{T}{N}\sum_q\sum_m \tilde{G}_{11}^\sigma(q, i\omega_m)\lambda_{11}(q, k-q \mid i\omega_n - i\omega_m), \tag{41}$$

$$\tilde{\Sigma}_{12}^\sigma(k, i\omega_n) =$$

$$= -\frac{T}{N}\sum_q\sum_m \tilde{G}_{12}^\sigma(q, i\omega_m)\lambda_{12}(q, k-q \mid i\omega_n - i\omega_m). \tag{42}$$

The interaction functions are given by

$$\lambda_{11}(q, k-q \mid i\omega_\nu) = g^2(q, k-q)D^+(k-q, i\omega_\nu) \,, \tag{43}$$

$$\lambda_{12}(q, k-q \mid i\omega_\nu) = g^2(q, k-q)D^-(k-q, i\omega_\nu). \tag{44}$$

To calculate superconducting T_c it is sufficient to study a linearized system of the Eliashberg equations (39) which has the following form

$$\tilde{G}_{11}^\sigma(k, i\Omega_n) = \frac{1}{i\omega_n - E_k + \tilde{\mu} - \tilde{\Sigma}_{11}^\sigma(k, i\omega_n)}, \tag{45}$$

$$\Phi^\sigma(k, i\omega_n) = \Delta_k^\sigma + \phi^\sigma(k, i\omega_n)$$

$$= \frac{T}{N}\sum_q\sum_m \{J(k-q) + \lambda_{12}(q, k-q \mid i\omega_n - i\omega_m)\}$$

$$\times \tilde{G}_{11}^\sigma(q, i\omega_m)\tilde{G}_{11}^{\bar{\sigma}}(q, -i\omega_m)\Phi^\sigma(q, i\omega_m). \tag{46}$$

At first the system of equations for the normal GF (45), (41) was solved numerically for a given concentration of electrons

$$\frac{n}{1 - n/2} = \frac{1}{N}\sum_{k,\sigma} N_{k\sigma} = 1 + \frac{2T}{N}\sum_k \sum_{n=-\infty}^{\infty} \tilde{G}_{11}(k, i\omega_n) \,. \tag{47}$$

Then the eigenvalues and eigenfunctions of the gap function (46) were calculated to obtain the superconducting transition temperature T_c and the $(\mathbf{k}, \omega)$-dependence of the gap function.

For numerical calculations we take into account only the spin-fluctuation contribution and write the function $D_s^\pm(q, i\omega_\nu)$ (37) in the form

$$D_s^\pm(q, i\omega_\nu) = \langle\langle \mathbf{S}_q \mid \mathbf{S}_{-q}\rangle\rangle_{i\omega_\nu} = -\int_0^{+\infty} \frac{2z dz}{z^2 + \omega_\nu^2}\chi_s''(q, z). \tag{48}$$

For the spin-fluctuation susceptibility we used a model representation suggested in numerical studies [47, 48]

$$\chi_s''(q, \omega) = -\frac{1}{\pi}\mathrm{Im}\,\langle\langle \mathbf{S}_q \mid \mathbf{S}_{-q}\rangle\rangle_{\omega + i\delta} = \chi_s(q)\,\chi_s''(\omega)$$

$$= \frac{\chi_0}{1 + \xi^2(1 + \gamma(q))}\,\tanh\frac{\omega}{2T}\frac{1}{1 + (\omega/\omega_s)^2}, \tag{49}$$

with characteristic AFM correlation length ξ and spin-fluctuation energy $\omega_s \simeq J$. However, the q-dependent part we took in a slightly different form, as a periodic function in q-space with more extended maxima at $(\pm\pi, \pm\pi)$ points. To fix the constant χ_0 in (49) we use the following normalization condition

$$\frac{1}{N}\sum_i \langle \mathbf{S}_i \mathbf{S}_i\rangle = \frac{1}{N}\sum_q \chi_s(q)\int_{-\infty}^{+\infty}\frac{dz}{\exp(z/T) - 1}\chi_s''(z)$$

$$= \frac{\pi\omega_s}{2N}\sum_q \chi_s(q) = \frac{3}{4}n, \tag{50}$$

which gives

$$\chi_0 = \frac{3n}{2\pi\omega_s C_1}, \quad C_1 = \frac{1}{N}\sum_q \frac{1}{1 + \xi^2(1 + \gamma(q))}.$$

In the approximation (48) we get for the interaction functions (43), (44)

$$\lambda_{11}(q, k-q \mid i\omega_\nu) = \lambda_{12}(q, k-q \mid i\omega_\nu)$$

$$= -g^2(q, k-q)\chi_s(k-q)F_s(i\omega_\nu), \tag{51}$$

where

$$F_s(\omega_\nu) = \int_0^\infty \frac{2xdx}{x^2 + (\omega_\nu/\omega_s)^2}\frac{1}{1+x^2}\tanh\frac{x}{2\tau} \tag{52}$$

is the spectral function, $\tau = T/\omega_s$. Within the model (49) the static spin correlation functions (28) read:

$$\chi_{1s} = \langle \mathbf{S}_i\mathbf{S}_{i+a_1}\rangle = \frac{1}{N}\sum_q \gamma(q)\langle \mathbf{S}_q\mathbf{S}_{-q}\rangle,$$

$$\chi_{2s} = \langle \mathbf{S}_i\mathbf{S}_{i+a_2}\rangle = \frac{1}{N}\sum_q \gamma'(q)\langle \mathbf{S}_q\mathbf{S}_{-q}\rangle\,, \tag{53}$$

where $\langle \mathbf{S}_q\mathbf{S}_{-q}\rangle = (\pi\omega_s/2)\chi_s(q)$.

To analyze a role of different interactions in the electron - spin-fluctuation scattering in (51) we consider the weak coupling approximation for the Eliashberg equation (38). It is given by the following approximation for the interaction (51) [49]:

$$\lambda_{12}(q, k-q \mid i\omega_n - i\omega_m)$$

$$\simeq -\lambda(q, k-q)\theta(\omega_s - |\omega_n|)\theta(\omega_s - |\omega_m|), \tag{54}$$

where we take $F_s(\omega_\nu) \simeq F_s(\omega_s) \simeq 1$ and introduce

$$\lambda(q, k-q) = g^2(q, k-q)\chi_s(k-q). \tag{55}$$

In the weak coupling limit we have for the anomalous GF:

$$\tilde{G}^\sigma_{12}(k, i\omega_m) \simeq -\frac{\Phi^\sigma_k}{(\omega_m)^2 + (\Omega^\sigma_k)^2}\,, \tag{56}$$

where $\Omega^2_k = (E^\sigma_k + \xi^\sigma_k(0) - \tilde{\mu})^2 + \mid \Phi^\sigma_k \mid^2$ is the QP energy in the superconducting state with the frequency independent gap function Φ^σ_k. By performing summation over m in Eq.(42), we get the weak coupling BCS equation

$$\Phi^\sigma(k) = \frac{1}{N}\sum_q \{J(k-q) - \lambda(q, k-q)\}\frac{\Phi^\sigma_q}{2\Omega_q}\tanh\frac{\Omega_q}{2T}. \tag{57}$$

In comparison with the results of the diagram technique [26], in Eq. (57) the kinematical interaction is also included in the effective coupling constant of the second order (55). The equation for the gap function obtained in the MFA approximation within the diagram technique in [27] is given by Eq. (57) with $\lambda(q, k-q) = 0$ while the equation obtained in [28] has an additional factor $Q = 1 - n/2$ which is spurious as was shown in [23] (compare with [22]). Below we compare results for the superconducting T_c calculated in the weak coupling limit, Eq.(57), and obtained within

the Eliashberg equation (46) and study the role of the kinematical interaction in $\lambda(q, k-q)$.

The numerical calculations were performed using the fast Fourier transformation [50] for a 32×32 cluster. In the summation over the Matsubara frequencies we used up to 700 points with the constant cut-off $\omega_{max} = 20\ t$. Usually 10 – 30 iterations were needed to obtain a solution for the self-energy with an accuracy of order 0.001. The Padé approximation was used to calculate the one-electron spectral function $A_{11}(k, \omega)$ (33) and the density of states

$$A(\omega) = \frac{1}{N}\sum_k A^\sigma_{11}(k, \omega) \tag{58}$$

on the real frequency axis.

The calculations were performed for several values of the $t-J$ model parameters (J/t, t'/t), the AFM correlation length ξ in the model function (49) with $\omega_s = J$, and the hole concentration $\delta = 1 - n$. Below we present results for $\delta = 0.1 - 0.4$ and $\xi = 1,\ 3$ for the parameters $J = 0.4$, $t' = 0$ if other values are not indicated. All the energies and temperature are measured in units of t. To mimic suppression of AFM correlations with doping we usually take $\xi = 3$ for $\delta = 0.1$ and keep $\xi = 1$ for $\delta = 0.2 - 0.4$. Temperature effects are rather small for $T \leq 0.1$ and therefore we present only results for $T = 0.0125$.

4.1 Normal state

Results for the electron spectral density in the normal state, $A(k, \omega) = A_{11}(k, \omega)$ (33), are shown along the three symmetry directions in the BZ: $\Gamma(0,0) \to X(\pi, 0) \to M(\pi, \pi) \to \Gamma$ in Fig. 1 for $\delta = 0.1$, $\xi = 3$, Fig. 2 for $\delta = 0.4$, $\xi = 1$. For small concentration of holes, $\delta = 0.1$, we observe quite narrow QP peaks at the wave vectors crossing the Fermi surface (FS) along $M \to X$ and $M \to \Gamma$ directions. Along $X \to \Gamma$ direction wave vectors are below the FS (see Fig. 7.) and there are no QP peaks. In addition to the QP dispersion we see also a band of incoherent excitations with large dispersion below the Fermi energy, $\omega < 0$. The incoherent band is caused by the self-energy contribution peaked at the AFM wave vector ("shadow bands"). For $\xi = 3$ in Fig. 1 the incoherent band has a higher intensity due to stronger spin-fluctuations weight at the AFM wave vector . With increasing hole concentration the dispersion of the QP band also increases and the intensity of QP peaks are enhanced as shown in Fig. 2 for $\delta = 0.4$, $\xi = 1$. At the same time the intensity of the incoherent excitations are suppressed: the "high-energy feature" below the Fermi energy at the X point for $\delta = 0.1$, $\xi = 3$ in Fig. 1 practically disappears for $\delta = 0.4$, $\xi = 1$ in Fig. 2. As was discussed by Shen and Schrieffer [51] (see also [52]), the doping dependence of the spectral lineshape near $(\pi, 0)$ point can be explained by strong coupling of the QP hole excitations with collective excitations. In our model the latter are spin fluctuations which intensity at $(\pi.\pi)$ point is proportional

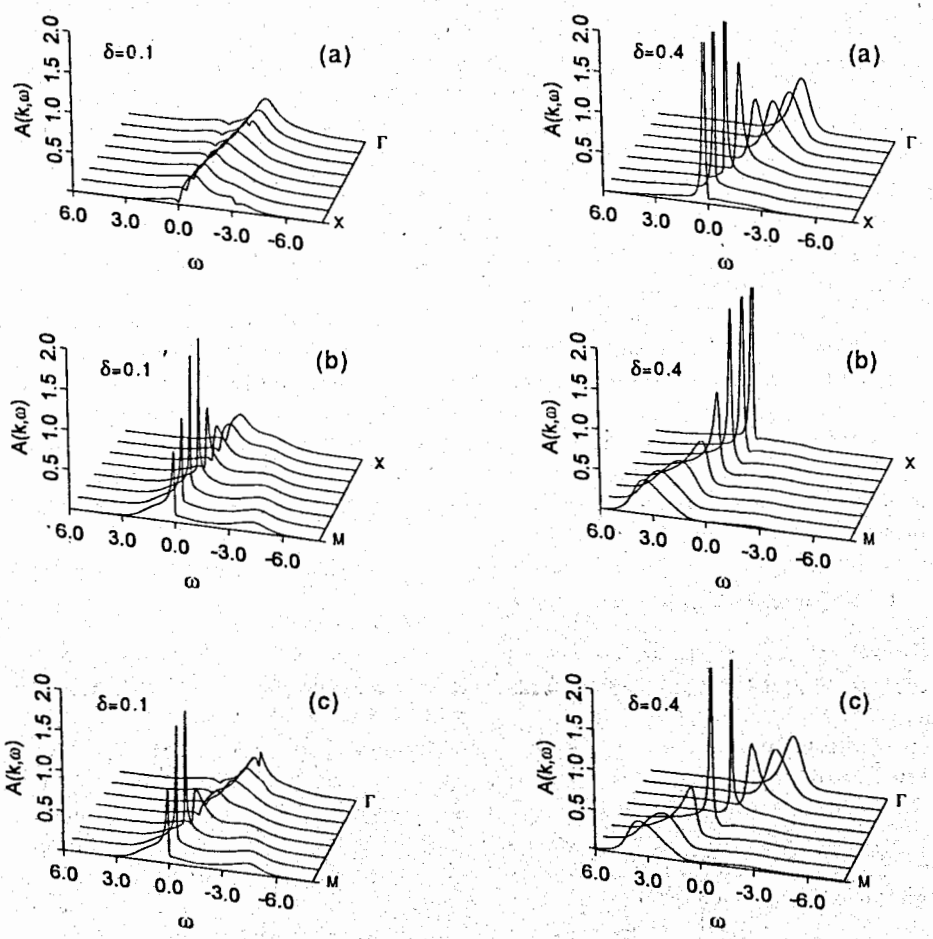

Fig. 1. Electron spectral density $A(k,\omega)$ for $\delta = 0.1$ and $\xi = 3$.
Fig. 2. Electron spectral density $A(k,\omega)$ for $\delta = 0.4$ and $\xi = 1$.

to ξ^2 (see Eq. (49)) resulting in strong suppression of the incoherent excitations with decreasing ξ and increasing δ. An important role of the next neighbor hopping t' in the explanation of the doping dependence of the spectral lineshape near $(\pi, 0)$ was also pointed out in [53].

These conclusions are supported by the doping dependence of the imaginary part of the self-energy $-\mathrm{Im}\Sigma(k,\omega) = -\mathrm{Im}\tilde{\Sigma}^{\sigma}_{11}(k,\omega+i\epsilon)$ shown in Fig. 3 for $\delta = 0.1$, $\xi = 3$ and Fig. 4 for $\delta = 0.3$, $\xi = 1$. With increasing hole concentration and decreasing

AFM correlation length ξ the self-energy decreases due to suppression of electron scattering on spin-fluctuations. It is interesting to note that for the underdoped region, $\delta \leq 0.1$, $\mathrm{Im}\Sigma(k,\omega)$ for $T \leq \omega \leq J$ is approximately proportional to ω (see Fig. 3, especially M-point) while for the overdoped region, $\delta \geq 0.3$, for small ω we have $\mathrm{Im}\Sigma(k,\omega) \propto \omega^2$. However, our $(\mathbf{k},\omega)$ resolution is not high enough to prove a transition from the non-Fermi liquid to the Fermi-liquid behavior with doping. Our results for electron spectral functions generally are in accord with calculations [48] done for zero temperature. However, contrary to [48],we did not introduce any

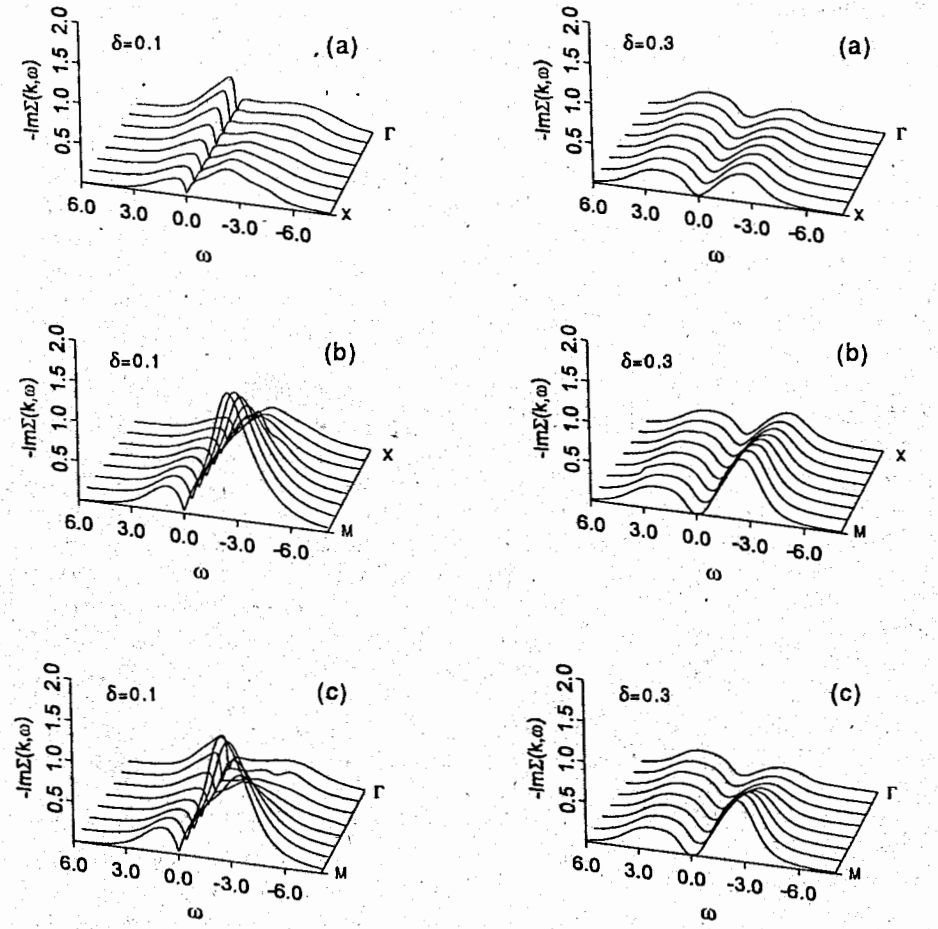

Fig. 3. Imaginary part of the electron self-energy $-\mathrm{Im}\tilde{\Sigma}^{\sigma}_{11}(k,\omega+i\epsilon)$ for $\delta = 0.1$ and $\xi = 3$.
Fig. 4. Imaginary part of the electron self-energy $-\mathrm{Im}\tilde{\Sigma}^{\sigma}_{11}(k,\omega+i\epsilon)$ for $\delta = 0.3$ and $\xi = 1$.

additional incoherent part for the self-energy (30) to fulfill the Luttinger theorem. We feel this fitting to be artificial. We find also a reasonable agreement of our results for the spectral function for $\delta = 0.1$, $\xi = 3$, including both the coherent QP dispersion and incoherent band, with the calculations in [42] within the exact-diagonalization technique for a finite cluster of 20 lattice sites with 2 holes ($\delta = 0.1$).

In Fig. 5 we show the QP dispersion $E(\mathbf{k})$ for $\delta = 0.1$, $\xi = 3$ and $t' = 0, \pm 0.1$ (upper panel) and $\delta = 0.1$, $\xi = 3$ and $\delta = 0.4$, $\xi = 1$ (lower panel) which are calculated from the maxima of spectral density. As we see, the QP band width strongly increases with doping while the next neighbor hopping t' change the dispersion mostly at $\Gamma(0,0)$ and $X(\pi,0)$ points. These results can be already explained within the spectrum E_k in MFA, Eq. (23). Being written in the form

$$E_k^\sigma = -4t\gamma(k)\, Q[1 + \chi_{1s}/Q^2] - 4t'\gamma'(k)\, Q[1 + \chi_{2s}/Q^2]$$
$$= -t_{eff}\, \gamma(k) - t'_{eff}\, \gamma'(k),$$

it shows a strong dependence of the effective hopping parameters on the static AFM correlation functions (28): $\chi_{1s} = \langle \mathbf{S}_i \mathbf{S}_{i+a_1} \rangle$, $\chi_{2s} = \langle \mathbf{S}_i \mathbf{S}_{i+a_2} \rangle$. For small hole concentration and large AFM correlation length, e.g., $\delta = 0.1$, $\xi = 3$, we have $\chi_{1s} = -0.23$, $\chi_{2s} = 0.13$ (see Table I) and $t_{eff} \simeq 0.53t$, $t'_{eff} \simeq 1.25t'$. At large hole concentration, e.g., $\delta = 0.4$, $\xi = 1$, we have $\chi_{1s} = -0.06$, $\chi_{2s} = 0.016$ and $t_{eff} \simeq 2.5t$, $t'_{eff} \simeq 2.7t'$. The self-energy additionally renormalizes the spectrum but the general δ, ξ dependence obtained in the MFA agrees quite well with the observed in Fig. 5.

Here we would like to point out that in the large-N expansion technique, both for the slave boson [12], [13] and the Baym-Kadanoff variational GF [16, 17], the narrowing of the band due to the discussed above AFM correlations is ignored. In the $1/N$ expansion the static spin correlation functions χ_{1s}, χ_{1s} appear to be of the higher order in $1/N$ and therefore are omitted. Moreover, the factor Q in the spectrum in the MFA, Eq. (23) is also underestimated. We have in Eq. (23) $Q_\sigma = \langle X_i^{00} + X_i^{\sigma\sigma} \rangle = (1+\delta)/2$ while in the $1/N$ expansion $Q = \langle X_i^{00} \rangle = \delta$ since the correlation function $\langle X_i^{\sigma\sigma} \rangle$ is of the order $1/N$ and is disregarded. These underestimation of the strong kinematical interaction in the large-N expansion changes the doping dependence of the QP spectrum in MFA in comparison with real situation with $N = 2$.

Figure 6 shows electron density of states $A(\omega)$ for $\delta = 0.1$, $\xi = 3$ (dashed line) and $\delta = 0.4$, $\xi = 1$ (solid line). Since the incoherent band is strongly suppressed at large hole concentration ($\delta = 0.4$) and small AFM correlation length ($\xi = 1$), the electron density of state has a nearly symmetric form with a broad band width (of the order of $7t$) in comparison with highly asymmetric one for low doping ($\delta = 0.1$) where high density of states below the Fermi level is due to the incoherent band. The obtained results for the spectral functions seem to prove a strong dressing of hole QP in the underdoped regime and weak coupling of electrons with spin fluctuations in the overdoped regime which are in accord with results of angle-resolved

photoemission spectroscopy [54].

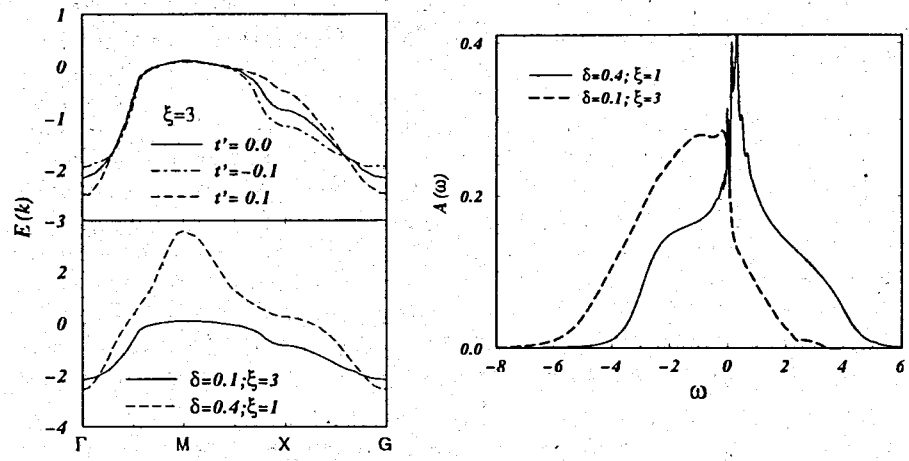

Fig. 5. Electron quasiparticle spectrum $E(\mathbf{k})$ for $\delta = 0.1$ and $t' = 0$, ± 0.1, $\xi = 3$ (upper panel), and $\delta = 0.1$, $\xi = 3$ (solid line) and $\delta = 0.4$, $\xi = 1$ (dashed line) (lower panel).
Fig. 6. Electron density of states $A(\omega)$ for $\delta = 0.1$, $\xi = 3$ (dashed line) and $\delta = 0.4$, $\xi = 1$ (solid line).

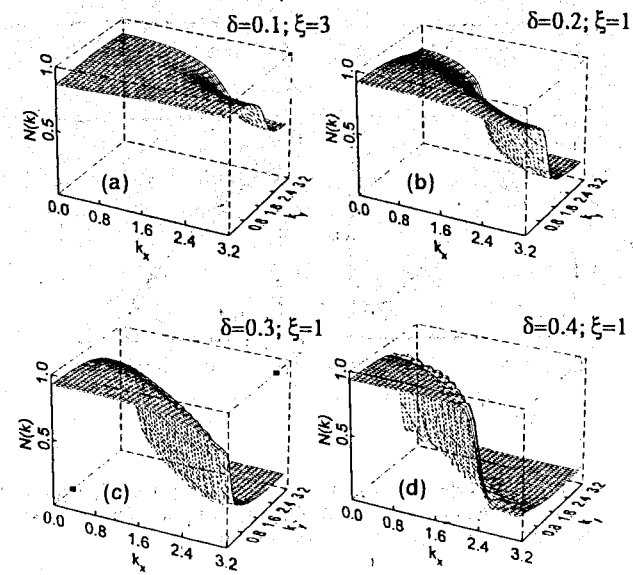

Fig. 7. Electron occupation numbers $N(\mathbf{k})$ versus $\mathbf{k}$, $(0 \le k_x, k_y \le \pi)$, for different hole concentration δ and AFM correlation length ξ: $\delta = 0.1$, $\xi = 3$ (a), $\delta = 0.2$, $\xi = 1$ (b), $\delta = 0.3$, $\xi = 1$ (c), $\delta = 0.4$, $\xi = 1$ (d).

Remarkable results were obtained for the electron occupation numbers (27) $n_{\mathbf{k},\sigma} = \langle X_k^{g0} X_k^{0\sigma} \rangle = [(1+\delta)/2]\, N_{\mathbf{k}\sigma}$. In Fig. 7 the function $N(\mathbf{k}) = N_{\mathbf{k}\sigma}$ is shown for different hole concentrations: (a) $\delta = 0.1$, $\xi = 3$, and (b)-(d) $\delta = 0.2 - 0.4$, $\xi = 1$. The shape of the FS changes from the hole-like around $M(\pi,\pi)$ point of BZ at small doping to the electron-like around $\Gamma(0,0)$ point of BZ for large doping. However, the drop of $N(\mathbf{k})$ at the FS is quite small, especially at small doping, which is a specific feature of strongly correlated electronic systems. Large occupation numbers throughout the BZ are due to the incoherent contribution in the spectral density $A(k,\omega)$ under the Fermi level (see Figs. 1 - 2). The maximal occupation numbers for electrons, $n_{\mathbf{k}} = (1 - n/2)\, N(\mathbf{k}) \leq 0.55$ for $\delta = 0.1$, agrees with the results of the exact-diagonalization technique for finite clusters [42]. The FS crosses the $(\pm\pi, 0)$, $(0, \pm\pi)$ points of BZ at $\delta \simeq 0.3$. The evolution of the FS with hole concentration is also shown in Fig. 8 by bold solid lines. The volume of the FS at

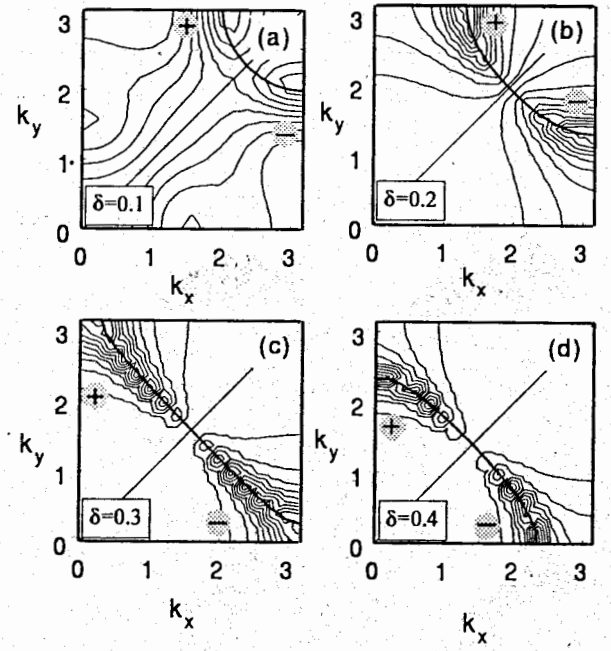

Fig. 8. The Fermi surface (bold solid lines) and the gap function $\Phi(\mathbf{k},0)$ (thin solid lines with (+) and (-) showing the sign of the gap) versus $\mathbf{k}$, $(0 \leq k_x, k_y \leq \pi)$, for different hole concentration δ and AFM correlation length ξ: $\delta = 0.1$, $\xi = 3$ (a), $\delta = 0.2$, $\xi = 1$ (b), $\delta = 0.3$, $\xi = 1$ (c), $\delta = 0.4$, $\xi = 1$ (d).

small doping is proportional to the hole concentrations, e.g., for $\delta = 0.1$, 0.2 the ratio of the BZ part for $k > k_F$ to the whole BZ are close to 10 % and 20 %,

respectively, while according to the Luttinger theorem the ratio should be equal to $(1+\delta)/2$. However, the problem of the Luttinger theorem for strongly correlated systems should be discussed for the Hubbard model where the weight transfer from the upper Hubbard subband to the lower one with doping is important and cannot be taken into account within the projected one-subband $t-J$ model (see, e.g., [55]).

4.2 Superconducting state .

The results of numerical solution of the linearized Eliashberg equation (46) are presented in Figs. 8 - 11. Figure 8 shows the contour plots in a quarter of BZ, $(0 \leq k_x, k_y \leq \pi)$, for the static gap function $\Phi(k) = \Phi(k, \omega = 0)$. At a small doping, $\delta = 0.1$, (Fig. 8 (a)), it has a more complicated k-dependence, with two positive and two negative maxima (shown by (+) and (-)) while at $\delta \geq 0.2$ only one positive and one negative maximum survive (Figs. 8 (b)-(d)). More clearly it is shown in Fig. 9 for $\Phi(k)$ in k-space for small concentration of holes, $\delta = 0.1$ (a), and for a nearly optimal one, $\delta = 0.3$ (b). The $\Phi(\mathbf{k})$-dependence has a complicated form that cannot be described by simple $(\cos k_x - \cos k_y)$ function usually used for the d-wave symmetry. However, in all cases the gap function obeys the B_{1g} symmetry: $\Phi(k_x, k_y) = -\Phi(k_y, k_x)$ which breaks the 4-fold symmetry of the FS in $\mathbf{k}$-space.

In Fig. 10 we present the superconducting T_c versus hole concentration δ for AFM correlation length $\xi = 1$ (solid line) and $\xi = 3$ (dashed line) obtained from numerical solution of Eq. (46). With increasing AFM correlation length ξ effective electron-electron coupling $\lambda_{12}(q, k-q \mid i\omega_\nu)$ mediated by spin fluctuations $\chi_s(k-q)$ also increases that rises T_c. For comparison, in Fig. 11 we present also superconducting temperature T_c versus hole concentration δ for AFM correlation length $\xi = 1$ in the weak coupling approximation, Eq.(57), for the full vertex, $J(k-q) - \lambda(q, k-q)$ (solid line), the vertex with $t(q) = 0$ in $\lambda(q, k-q)$ (dashed line), and in the MFA with $\lambda(q, k-q) = 0$ (dotted line). We see that in the weak coupling approximation T_c is much higher in comparison with that one obtained from the frequency-dependent equation (46) for the same static susceptibility, i.e., $\xi = 1$ in Eq. (49). However, the most important contribution in the weak coupling approximation gives the vertex in MFA, i.e. $J(k-q)$ in Eq. (57). The second order contribution, $\lambda(q, k-q) = g^2(q, k-q)\chi_s(k-q)$, enhances T_c both due to kinematical, $t(q)$, and exchange, $J(k-q)$, interactions. For larger AFM correlation length superconducting T_c is greatly enhanced in the weak coupling approximation, e.g. $T_c \simeq 0.1$ for $\xi = 3$.

So our calculations, done for the paramagnetic state in the $t-J$ model, confirm the results of the d-wave superconducting pairing with quite high T_c obtained within the spin-polaron $t-J$ model [40]. Contrary to the latter model, having the long-range AFM order, we obtain quite a high value of $T_c \simeq 0.01 - 0.04 \simeq 50 - 200$ K

for small AFM correlation length $\xi = 1 - 3$.

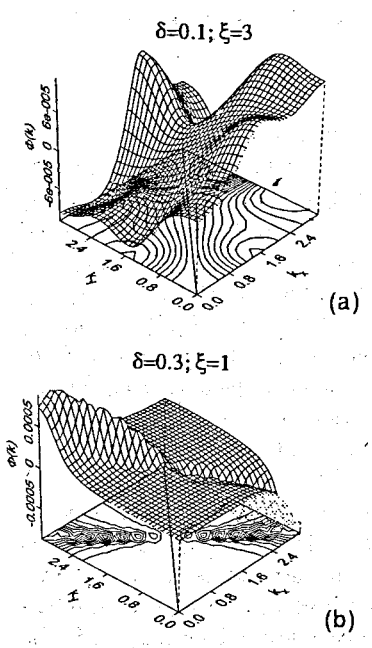

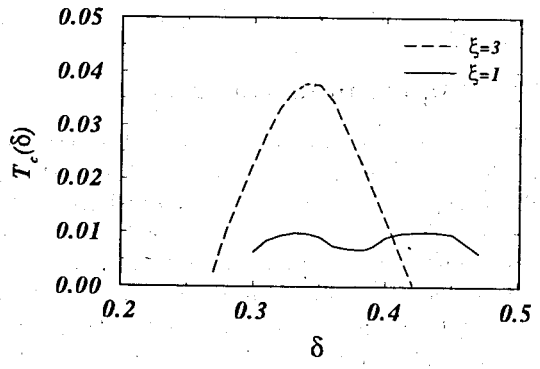

Fig. 10. The superconducting temperature T_c versus hole concentration δ for AFM correlation length $\xi = 1$ (solid line) and $\xi = 3$ (dashed line), obtained from Eq. (46).

Fig. 9. The gap function $\Phi(\mathbf{k}, \omega = 0)$ versus $\mathbf{k}$ for $\delta = 0.1$, $\xi = 3$ (a), $\delta = 0.2$, $\xi = 1$ (b).

To elucidate the role of AFM short-range fluctuations in the model and particular, strong dependence of T_c on the AFM correlation length ξ, obtained both within the full equation (46) and in the weak coupling limit (57), we present in Table I ξ-dependence of the static correlation functions, χ_{1s}, χ_{2s}, and the constant χ_0 in Eq. (49). The latter, as well the ratio $\chi_s(Q)/\chi_s(q=0)$, estimates the electron-spin fluctuation coupling while the static correlation functions χ_{1s}, χ_{2s}, Eq. (53), define the band width in the MFA, Eq. (23) as discussed above. Large increase of these parameters seen in Table I, with increasing ξ from their values at $\xi = 1$, explains strong changes in the spectral functions $A(k, \omega)$ and T_c. To analyze unconventional (k, ω)-dependence of the gap function we consider the kernel in the integral equation for the gap, Eq. (46), given by

$$K(q, k-q \mid \omega_\nu) = J(k-q) + \lambda_{12}(q, k-q \mid i\omega_\nu)$$
$$= J(k-q) - g^2(q, k-q)\chi_s(k-q)F_s(\omega_\nu). \qquad (59)$$

For the d-wave gap symmetry we can analyze only its q-dependence given by the projection:

$$\tilde{K}(q, \omega_\nu) = \frac{1}{N}\sum_k (\cos k_x - \cos k_y) K(q, k-q \mid \omega_\nu)$$
$$= (\cos q_x - \cos q_y)\, J - F_s(\omega_\nu) B(q_x, q_y), \qquad (60)$$

where

$$B(q_x, q_y) = \frac{1}{N}\sum_k (\cos k_x - \cos k_y) g^2(q, k-q)\chi_s(k-q). \qquad (61)$$

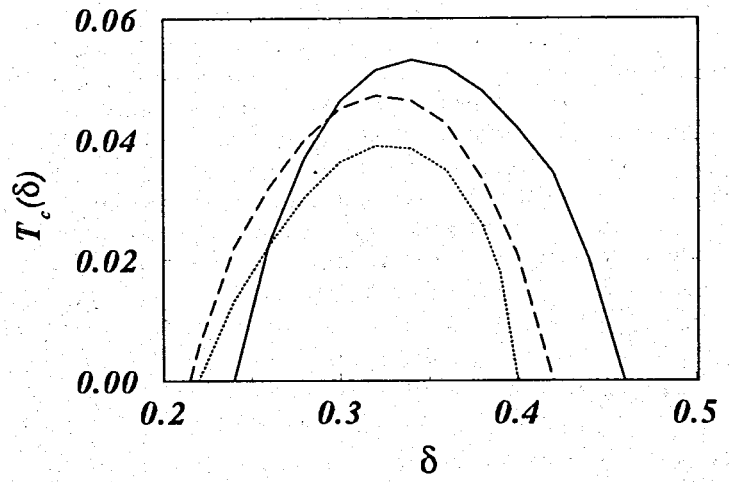

Fig. 11. The superconducting temperature T_c versus hole concentration δ for AFM correlation length $\xi = 1$ in the weak coupling approximation, Eq. (57), for the full vertex (solid line), the vertex with $t(q) = 0$ (dashed line), and in the MFA with $\lambda(q, k-q) = 0$ (dotted line).

Table I. Static spin correlations versus AFM correlation length ξ at different hole concentration δ.

ξ	δ	χ_0	χ_{1s}	χ_{2s}	$\chi_s(Q)/\chi_s(0)$
1	0.30	1.56	-0.072	0.019	3
3	0.10	7.40	-0.230	0.130	19
5	0.05	17.08	-0.311	0.213	51

The spectral function $F_s(\omega_\nu)(52)$ being large for low temperature $\tau = T/\omega_s \ll 1$ at $\omega_\nu = \omega_n - \omega_m = 0$ $(F_s(\omega_s) \simeq 1)$ tends to zero for $\omega_\nu/\omega_s \gg 1$. Since the susceptibility $\chi_s(k-q)$ is peaked at $k - q = (\pi, \pi)$ we can further approximate the sum in Eq. (61) by

$$B(q_x, q_y) \simeq -(\cos q_x - \cos q_y)[t(q) + 2J]^2 \frac{1}{N} \sum_k \chi_s(k-q)$$

$$\simeq (\cos q_x - \cos q_y)[t(q) + 2J]^2 \chi_0 \,. \qquad (62)$$

Therefore the full projected kernel in the gap equation for the d-wave pairing in Eq. (46) is estimated by

$$\tilde{K}(q, \omega_\nu) \simeq (\cos q_x - \cos q_y)\{J + [t(q) + 2J]^2 \chi_0 \, F_s(\omega_\nu)\} \,. \qquad (63)$$

The same estimation holds for the weak coupling approximation (57) with $F_s(\omega_\nu) \simeq 1$. The kernel gives no contribution along the lines $|q_x| = |q_y|$, as it should be for the d-wave pairing, while the kinematical interaction $t(q)$ vanishes along the lines $|q_x| + |q_y| = \pi$. Therefore, the pairing interaction should strongly depend on hole concentration being large when FS crosses the maxima of the kernel (60) in q-space. For the "optimal" doping the FS is close to the lines $|q_x| + |q_y| = \pi$ and the largest kinematical interaction gives no contribution. The very complicated behavior of the kernel in q-space (also influencing the gap ω-dependence) can explain unconventional $\mathbf{k}$ (and ω) dependence of the gap function. A small minimum for T_c in Fig. 10 at $\xi = 1$ for $\delta \simeq 0.37$ could be due to suppression of the kinematic interaction in the kernel (63) as discussed above.

5 CONCLUSIONS

In the present paper a theory of electron spectrum and superconducting pairing in the $t - t' - J$ model (7) in a paramagnetic state is proposed. By employing the equation of motion method for the two-time GF [43] and projection technique [25] we obtained the self-consistent system of equations for the matrix GF (38) and the self-energy (30), (31) in the noncrossing approximation, Eq. (29). Our equation for the gap function (46) in comparison with the diagram technique [26] has an additional contribution due to the kinematical interaction in the second order which enhances the d-wave pairing.

The analytical calculations were performed in the real time representation though the imaginary frequency technique was employed for numerical study of the linearized system of Eliashberg equations (45), (46). A model dynamic spin susceptibility (49) suggested in numerical studies [47, 48] was used for the calculations. The results for the electron spectral density (see Figs. 1-2) show QP excitations at the FS crossing and a dispersive incoherent band. For small hole concentration the QP dispersion is small while the intensity of the incoherent band is quite large. With doping the QP band width strongly increases and the incoherent band is suppressed. The results for single-electron spectral functions are in general agreement with the studies within exact-diagonalization technique [42] and compatible with ARPES investigations [54]. However, we have not tried to fit our single-hole QP dispersion to

experimental curves restricting ourselves to the simple version of the $t - J$ model with only one dimensionless parameter J/t (for discussion of the fitting problem see, e.g., [35] - [37]).

The occupation numbers $N(\mathbf{k})$ have the characteristic behavior for strongly correlated systems, Fig. 7. Being large throughout the BZ they show only a small drop at the FS. The volume of the FS at small doping is proportional to the hole concentration δ, as shown in Fig. 8, that does not obey the Luttinger theorem.

The superconducting pairing due to the exchange and the kinematic interactions (in the second order) has the d-wave symmetry, Fig. 9, and high T_c, Fig. 10. In the weak coupling approximation, Eq. (57), much larger T_c is observed, Fig. 11. Our calculations confirm the results of the d-wave superconducting pairing obtained within the spin-polaron $t - J$ model [40]. The advantage of the proposed microscopical theory of the d-wave spin-fluctuation superconducting pairing, in comparison with phenomenological approaches based on the Fermi liquid models close to AFM instability, is that we have used only two basic parameters for the model, the hopping energy, t, and the (super)exchange energy, J, which are characteristic to strongly correlated systems [56] and bring about the electron - spin-fluctuation interaction due to kinematical and exchange interactions.

In the noncrossing approximation (29) vertex corrections are disregarded as in the diagram technique in [26]. We think that vertex corrections should not change the main conclusions of our calculations. At least, we can argue that in our approach, where the model spin susceptibility (49) with small AFM correlation length, $\xi = 1-3$, is used, the vertex renormalization, estimated as $\chi_s(Q)/\chi_s(0)$ (see [57]), should not be large (see Table I).

However, the theory is still not fully self-consistent in that respect that a phenomenological model for spin-fluctuations has been used, Eq. (49), to enable a numerical study of temperature and doping dependence of one-electron spectrum and superconducting pairing. We are planning to perform fully self-consistent calculations by employing results for a dynamical spin susceptibility in the $t-J$ model [58] and to generalize our calculations for the asymmetric $(p-d)$ Hubbard model [55, 59].

Acknowledgments

We gratefully acknowledge stimulating discussions with P. Horsch, R. Zeyher, and A. Liechtenstein. We are also indebted to G. Jackeli and V. Yushankhai for valuable discussions and remarks. One of the authors (N.P.) thanks Prof. P. Fulde for the hospitality extended to him during his stay at the MPIPKS where a major part of the work has been done. We acknowledge usage of computational facilities of the Max-Planck-Institute in Stuttgart kindly provided for us by Prof. L. Hedin. Partial financial support by the INTAS–RFBR Program, Grant No 95–591 and by NREL, Subcontract AAX-6-16763-01 are acknowledged.

References

[1] N.M. Plakida *High-temperature superconductivity* (Springer-Verlag, Berlin, 1995).

[2] P.W. Anderson, Science **235**, 1196 (1987).

[3] P.W. Anderson, *The theory of superconductivity in the high-T_c cuprates* (Princeton University Press, Princeton, New Jersey, 1997).

[4] D.J. Scalapino, Phys. Reports **250**, 329 (1995).

[5] Th. Pruschke, M. Jarrell, and J.K. Freericks, Advance in Phys. **44**, 187 (1995).

[6] A. Georges, G. Kotliar, W. Krauth, and M. Rozenberg, Rev. Mod. Phys. **68**, 13 (1996).

[7] E. Dagotto, Rev. Mod. Phys. **66**, 763 (1994).

[8] Shiwei Zhang, J. Carlson, and J.E. Gubernatis, Phys. Rev. Lett., **78**, 4486 (1997).

[9] M.Yu. Kagan and T.M. Rice, J. Phys.: Condens. Matter **3**, 5373 (1994).

[10] E.S. Heeb and T.M. Rice, Europhys. Lett., **27**, 673 (1994).

[11] Y. Suzumura,Y. Hasegawa, and H. Fukuyama, J. Phys. Soc. Jpn. **57**, 401 (1988).

[12] G. Kotliar and J. Liu, Phys. Rev. Lett. **61**, 1784 (1988).

[13] M. Grilli and G. Kotliar, Phys. Rev. Lett. **64**, 1170 (1990).

[14] E. Arrigoni, C. Castellani, M. Grilli, R. Raimondi, G.C. Strinati, Phys. Rep. **241**, 291 (1994).

[15] A.E. Ruckenstein and S. Schmitt-Rink, Phys. Rev. B **38**, 7138 (1988).

[16] A. Greco and R. Zeyher, Europhys. Lett., **35**, 115 (1996).

[17] R. Zeyher and A. Greco, Z. Physik B **104**, 737 (1997), and to be published.

[18] R.O. Zaitsev, Sov. Phys. JETP **43**, 574 (1976).

[19] Yu.A. Izyumov and Yu.N. Scryabin, *Statistical Mechanics of Magnetically ordered systems* (Consultant Bureau, New York, 1989).

[20] R.O. Zaitsev and V.A. Ivanov, Fiz. Tver. Tela. **29**, 2554, 3111 (1987); Int. J. Mod. Phys. B **5**, 153 (1988); Physica C **153-155**, 1295 (1988).

[21] N.M. Plakida and I.V. Stasyuk, Modern Phys. Lett. **2** 969, (1988).

[22] N.N. Bogoliubov, V.L. Aksenov, and N.M. Plakida, Physica C, **153-155**, 99 (1988).

[23] N.M. Plakida, V.Yu. Yushankhai, and I.V. Stasyuk, Physica C, **160**, 80 (1989).

[24] V.Yu. Yushankhai, N.M. Plakida, and P. Kalinay, Physica C, **174**, 401 (1991).

[25] N.M. Plakida, Phys. Lett. A, **43**, 481 (1973).

[26] Yu.A. Izyumov and B.M. Letfulov, J. Phys.: Condens. Matter, **3** 5373 (1991).

[27] I.S. Sandalov and M. Richter, Phys. Rev. B **50**, 12855 (1994).

[28] F. Onufrieva, S. Petit, and Y. Sidis, Phys. Rev. B **54**, 12464 (1996).

[29] S. Schmitt-Rink, C.M. Varma, and A.E. Ruckenstein, Phys. Rev. Lett. **60**, 2793 (1988).

[30] C.L. Kane, P.A. Lee, and N. Read, Phys. Rev. B **39**, 6880 (1989).

[31] G. Martinez and P. Horsch, Phys. Rev. B, **44**, 317 (1991).

[32] Z. Liu and E. Manousakis, Phys. Rev. B **45**, 2425 (1992).

[33] A. Scherman A. and M. Schreiber, Phys. Rev. B, **48**, 7492 (1993); *ibid.* **50**, 12887 (1994).

[34] N.M. Plakida, V.S. Oudovenko, and V.Yu. Yushankhai, Phys. Rev. B **50**, 6431 (1994).

[35] J. Bala, A. Oleś, and J. Zaanen, Phys. Rev. B, **52**, 4597 (1995).

[36] V.I. Belinicher, A.I. Chernyshev, and V.A. Shubin, Phys. Rev. B **53**, 335 (1996), *ibid* **54**, 14914 (1996).

[37] V.Yu. Yushankhai, V.S. Oudovenko, and R. Hayn, Phys. Rev. B **55**, 15562 (1997).

[38] E. Dagotto, A. Nazarenko, and A. Moreo, Phys. Rev. Lett. **74**, 310 (1995).

[39] V.I. Belinicher, A.L. Chernyshev, A.V. Dotsenko, and O.P. Sushkov, Phys. Rev. B **51**, 6076 (1995).

[40] N.M. Plakida, V.S. Oudovenko, P. Horsch, and A.I. Liechtenstein, Phys. Rev. B**55**, R11997 (1997).

[41] A. Scherman and M. Schreiber, Phys. Rev. B, **52**, 10621 (1995).

[42] W. Stephan and P. Horsch, Phys. Rev. Lett. **66**, 2258 (1991).

[43] D.N. Zubarev, Sov. Phys. Usp. **3**, 320 (1960).

[44] F.C.Zhang and T.M. Rice, Phys. Rev. B, **37**, 3759 (1988).

[45] J. Hubbard, Proc. Roy. Soc. A **285**, 542 (1965).

[46] L.F. Feiner, J.H. Jefferson, and R. Raimondi, Phys. Rev. B, **53**, 8751 (1996).

[47] J. Jaklič and P. Prelovšek, Phys. Rev. Lett. **74**, 3411 (1995); *ibid.* **75**, 1340 (1995).

[48] P. Prelovšek, Z. Physik B **103**, 363 (1997).

[49] Ph. Allen and B. Mitrović, Solid State Physics, vol. **37**, 1-92 (1982).

[50] J.W. Serene and D.W. Hess, Phys. Rev. B, **44**, 3391 (1991).

[51] Z.-X. Shen and J.R. Schrieffer, Phys. Rev. Lett. **78**, 1771 (1997).

[52] J. Schmalian, D. Pines, and B. Stojković, Phys. Rev. Lett. **80**, 3839 (1998).

[53] C. Kim, P.J. White, Z.-X. Shen, *et al.*, Phys. Rev. Lett. **80**, 4245 (1998).

[54] For a review, see Z.-X. Shen and D.S. Dessau, Phys. Rep. **253**, 1-161 (1995).

[55] N.M. Plakida, R. Hayn, and J.-L. Richard, Phys. Rev. B **51**, 16599 (1995).

[56] P.W. Anderson, Adv. in Phys. **46**, 3 (1997).

[57] J.R. Schrieffer, J. Low Temp. Phys. **99**, 397 (1995).

[58] G. Jackeli and N.M. Plakida, Theor. and Math. Phys. **114**, 426 (1998).

[59] N.M. Plakida, Physica C **282-287**, 1737 (1997).

Received by Publishing Department
on August 21, 1998.

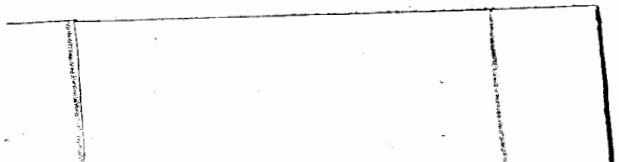

Плакида Н.М., Удовенко В.С. E17-98-244

Электронный спектр и сверхпроводимость в $t-J$ модели при умеренном допировании

Предложена микроскопическая теория для описания электронного спектра и сверхпроводимости в пределе сильных электронных корреляций. Мы рассматриваем двухмерную $t-J$ модель для парамагнитного состояния, используя проекционную технику для функций Грина от операторов Хаббарда. Самосогласованное численное решение уравнений Элиашберга выполнено в приближении непересекающихся диаграмм. Обменное и кинематическое взаимодействия электронов со спиновыми флуктуациями описываются динамической спиновой восприимчивостью с короткодействующими антиферромагнитными корреляциями. Структура одноэлектронной спектральной плотности представляет собой узкий квазичастичный пик у поверхности Ферми и широкую некогерентную часть ниже уровня Ферми. Квазичастичная дисперсия, будучи малой при малом допировании, становится большой при умеренном допировании. Поверхность Ферми при малой концентрации дырок δ имеет вид четырех «карманов» вокруг точек $(\pm\pi, \pm\pi)$, а при увеличении допирования переходит в большую электронную поверхность, которая пересекает точки зоны Бриллюэна $(\pm\pi, 0)$, $(0, \pm\pi)$ при допировании $\delta \simeq 0{,}3$. Числа заполнения $N(\mathbf{k})$ велики во всей зоне Бриллюэна, проявляя небольшой скачок, увеличивающийся с допированием, на поверхности Ферми. Вычислена $(\mathbf{k}, \omega)$ зависимость сверхпроводящей щелевой функции и температура сверхпроводящего перехода T_c прямым численным решением линеаризованных уравнений Элиашберга. Мы получили d-волновую симметрию щелевой функции и $T_c \simeq 0{,}04t$ при оптимальном допировании $\delta \simeq 0{,}3$. Сверхпроводящее спаривание посредством спиновых флуктуаций обусловлено как обменным, так и кинематическим взаимодействием; последнее, будучи порядка t^2/J, дает основной вклад.

Работа выполнена в Лаборатории теоретической физики им. Н.Н.Боголюбова ОИЯИ.
Препринт Объединенного института ядерных исследований. Дубна, 1998

Plakida N.M., Oudovenko V.S. E17-98-244

Electron Spectrum and Superconductivity in the $t-J$ Model at Moderate Doping

A microscopical theory of electron spectrum and superconductivity in the limit of strong electron correlations is formulated. We consider the two-dimensional $t-J$ model in a paramagnetic state by employing a projection technique for the Green functions in terms of the Hubbard operators. A self-consistent numerical solution of Eliashberg equations is performed in the noncrossing approximation. Exchange and kinematical interactions of electrons with spin fluctuations are described by a dynamical spin susceptibility with short-range antiferromagnetic correlations. The one-electron spectral density reveals narrow quasiparticle (QP) peaks close to the Fermi surface (FS) with an additional broad incoherent band below the Fermi level. The QP dispersion, being small at low doping, $\delta < 0.1$, becomes large for moderate doping. The form of the FS changes from four hole pockets at $(\pm\pi, \pm\pi)$ points at low doping to a large electron-like one crossing the $(\pm\pi, 0)$, $(0, \pm\pi)$ points of the Brillouin zone (BZ) at $\delta \simeq 0.3$. The occupation numbers $N(\mathbf{k})$ are large throughout the BZ and show only a small drop, increasing with doping, at the FS. The $(\mathbf{k}, \omega)$-dependent superconducting gap function and T_c are calculated by a direct numerical solution of the linearized Eliashberg equations. We observe the d-wave symmetry of the gap and $T_c \simeq 0.04t$ at optimal fluctuations due to the exchange and kinematical interactions where the latter, being of the order t^2/J, gives a substantial contribution.

The investigation has been performed at the Bogoliubov Laboratory of Theoretical Physics, JINR.

Preprint of the Joint Institute for Nuclear Research. Dubna, 1998